Development of an inversion methodology, using heuristic method, applied to the Magnetotelluric Method with a pseudo 2D formulation

Daniel Silva de Oliveira, Cosme Ferreira da Ponte Neto (Observatório Nacional, Rio de Janeiro, Brazil)

This paper was prepared for presentation at the 15th International Congress of the Brazilian Geophysical Society, held in Rio de Janeiro, Brazil, 31 July to 3 August, 2017.

Abstract

In this work, an inversion methodology was developed for the 2D Magnetotelluric Method for a n-layer model. The proposed method is an extension of the 1D formulation for a model of horizontal and infinite layers. The inversion is performed through the simultaneous solution of all the stations of the profile using the genetic algorithm.

Introduction

We call telluric currents the variations of electric current inside the Earth. The electromagnetic geophysical method that associates these currents with the variations of Earth's magnetic field and provides information on the distribution of resistivity of the rocks in the subsurface is called Magnetotelluric (MT). The MT method originates in the works of Tikhonov (1950), Cagniard (1953) and Weidelt (1972). This is a passive method, i.e. the MT method uses Earth's natural electromagnetic fields, unlike active geoelectric techniques, in which a current source is injected into the ground, functioning as an artificial source (Simpson and Bahr, 2005). The MT method is applied to investigate subsurface geological structures with depths that can reach 500 km and is mainly used in studies involving stratification of the medium, geoelectric zoning, mapping of underground topography, detection of conductive zones in the Earth crust and upper mantle and recognition of deep faults (Berdichevsky and Dmitriev, 2010).The data acquisition is performed through the assembly of fixed stations where electrical and magnetic field measurements are performed simultaneously, where the stations must operate for a predetermined period, depending on the objectives of the study. The operation and assembly of the stations are low cost and do not cause significant environmental impact.

The usual procedure to develop a program for the solution of an inverse problem involves, firstly, the elaboration of a computational program for the forward model. This is due the need to produce synthetic data, wherewith the inversion program will initially work. In this way, two computational programs were developed: one for the forward model and the other for the inverse model, the latter using a heuristic method called Genetic Algorithm. Specifically, this work consists in the elaboration of a computational program that provides the solution of the inverse problem for the Magnetotelluric Method with a pseudo 2D formulation for a layer model, using as basis the 1D formulation of the model presented by Rijo, 2004. The synthetic data were inverted with all the stations simultaneously, and satisfactory results were obtained. After the tests with the synthetic data, data collected by the Observatório Nacional will be used in a profile of approximately 180 km containing 11 stations cutting the Parnaíba basin. These data have great scientific importance, since the Parnaíba basin presents geological characteristics compatible with the presence of hydrocarbons, which brings economic interest to this area. However, the Parnaíba basin is still little studied and works like this can contribute to a detailed study of the geological structures present there. This stage of the work is ongoing.

The Magnetotelluric Method

Using existing electromagnetic fields in nature to study the Earth's electrical structure, the MT method typically works with periods ranging from 10^{-5}s to 10^{5}s (Nunes, 2007). The portion of the geomagnetic field that varies with time and that induces the flow of currents on Earth are called magnetoteluric fields (Lugão, 1993). These variations can occur in intervals ranging from milliseconds (discarded by low penetration on the earth's surface), days, and even centuries. Measured signals with periods shorter than 1s are attributed to lightning strikes. Above 1s, the measured signals are attributed to the interaction between the solar wind and the terrestrial magnetosphere. From the MT method, we can measure the tangential components of the electric and magnetic fields at the desired point in subsurface. Combining equipment such as electrodes, magnetometers and induction coils, we can simultaneously record two components of the electric field (E_x e E_y) and three components of the magnetic field (H_x, H_y e H_z). Dipoles (electrodes at a distance of 50 to 100 m) are used, crossing them mutually, for the measurement of telluric channels. The electrodes measure the electric field in two horizontal orthogonal directions. The measurement is made by determining the potential difference between pairs of electrodes spaced from a known distance. Electrode pairs are usually placed in the north-south and east-west directions, arranged in the form of "X" or "L", the latter with an electrode shared between two orthogonal dipoles (Chave and Jones, 2012) . In order to measure the magnetic field components, three high sensitivity magnetic induction coils are used. With the help of a compass, the sensors should be aligned with the magnetic north.

Forward model formulation

We can obtain the curves of apparent resistivity ρ_a and phase ϕ for several frequencies ω from the determination of the impedance Z, obtained through the tensor relationship

$$\begin{pmatrix}E_x\\ E_y\end{pmatrix} = \begin{pmatrix}Z_{xx} & Z_{xy}\\ Z_{yx} & Z_{yy}\end{pmatrix}\begin{pmatrix}H_x\\ H_y\end{pmatrix} \tag{1}$$

or simply,

$$Z_{xy}(\omega) = \frac{E_x(\omega)}{H_y(\omega)} \tag{2}$$

in homogeneous semi-spaces.

The Impedance Tensor is part of an Earth model that describes a linear system whose input is the magnetic field H, and the output is the electric field E. This model is based on Maxwell's equations. Through the impedance tensor, it is possible to estimate the apparent resistivity ρ_a and phase ϕ, in 2D situations, through equations

$$\rho_{a,ij}(\omega) = \frac{|Z_{ij}(\omega)|^2}{\mu_0 \omega} \tag{3}$$

and

$$\phi_{ij} = tan^{-1}\left(\frac{Im[Z_{ij}]}{Re[Z_{ij}]}\right) \tag{4}$$

where $\mu_0 = 4\pi \times 10^{-7} H/m$.

Inverse Problem: Genetic Algorithm

Genetic Algorithms (GAs) are search algorithms based on the mechanics of natural selection, proposed by Charles Darwin. This type of algorithm has the ability to explore information obtained in previous iterations to speculate the best solution in the subsequent iterations, in search of the best performance (Goldberg, 1989). Each individual (treated here as a complete set of solutions), in this type of algorithm, receives an evaluation related to its potential as solution of the proposed problem. Based on this evaluation, genetic operators are applied, which consist of computational approximations for phenomena occurring in nature, such as sexual reproduction and mutation (Linden, 2006). These operators, especially the mutation, are responsible for one of the most prominent characteristics of GAs, which is that they have the capacity to leave a local minimum and have the possibility of finding a global minimum. This type of algorithm does not guarantee the optimal solution, but can get very close to it. The Genetic Algorithm we use, counts on an initial population (randomly chosen). Right after the draw, there is an adjustment, and if this adjustment gets a satisfactory solution, the program shows the best estimate and comes to an end. Otherwise, the program performs "choice of parents", which consists of choosing the best "individuals" (set of solutions) and crosses them right away (crossover). In this last step there is a small probability of mutation, pre-defined in the algorithm. Soon after, there is a new adjustment, and if the solution is satisfactory, the program shows the best estimate and comes to an end. Otherwise, the program re-enters the loop (new generation). At the end of each generation there is what we call "elitism," where the program "clones" the best individuals of the current generation and inserts them into the next generation. This process ensures that the best individuals of each generation will be in the next generation. A generic flowchart of a Genetic Algorithm is shown in Figure 1.

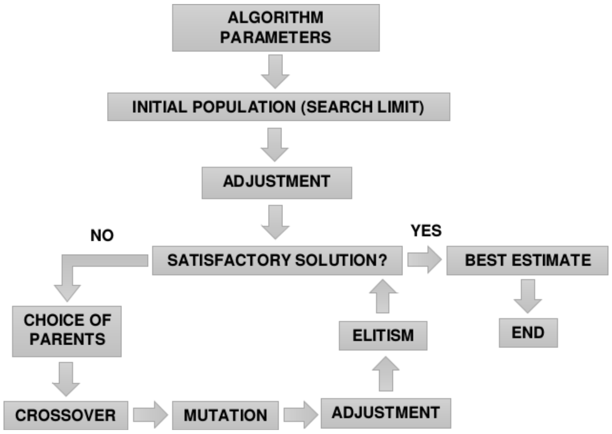

Figure 1: Flowchart of the Genetic Algorithm

Forward model description

Our model for MT survey considers a stratigraphic column consisting of five layers, based on the Rijo model. For the calculations, 26 periods between 0.01 and 1000 seconds, distributed evenly on a logarithmic scale were used (Rijo, 2004, p.28) . Table 1 shows the input data of our forward model, containing the position of each of the 6 stations, the thicknesses of each of the layers and the values of their respective resistivities. With the data in Table 1, the profile of the inverse model used was made, as shown in Figure 2. The red filled circles located at the top of the profile correspond to the positions of the six stations. The profile was built from left to right.

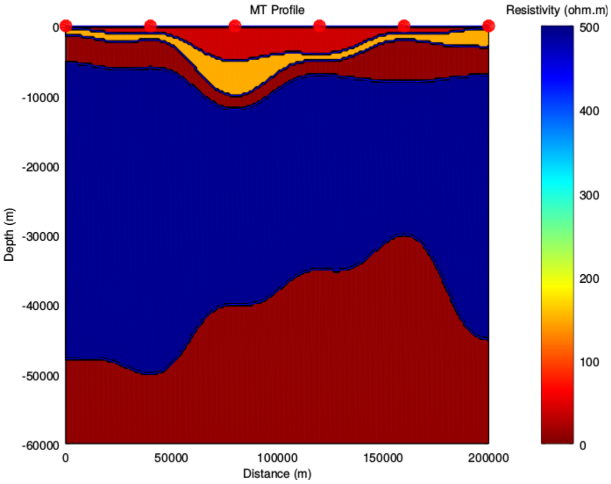

Figure 2: Profile of the forward model.

Results

The output parameters of the forward model (which are the input data of our inverse model) were contaminated with zero mean Gaussian noise and standard deviation of 2.66% for the apparent resistivity and 5.57% for the phase. An initial population of one hundred individuals were used. The search spaces used in the inversion were: Layer thickness 1 = [350, 5000]; Layer thickness 2 = [1000, 5000]; Layer thickness 3 = [2000, 6000]; Layer thickness 4 = [22000, 45000]; Resistivities = [5, 600]. The fit graphs of

Table 1: Forward model data.

		STATION 1	STATION 2	STATION 3	STATION 4	STATION 5	STATION 6
	HORIZONTAL COORDINATE (m)	0	40000	80000	120000	160000	200000
	RESISTIVITY $(\Omega.m)$	THICKNESS					
LAYER 1	40	350	1000	5000	4000	1000	400
LAYER 2	150	1000	1000	5000	1000	1000	2600
LAYER 3	10	4000	4000	2000	2000	6000	4100
LAYER 4	500	42500	44000	28000	28000	22000	37900
LAYER 5	10	∞	∞	∞	∞	∞	∞

all six stations are shown in Figure 3. There are two graphs for each station. The first showing the fit of the apparent resistivity versus the period, and the second showing the fit of the phase versus the period. The blue line shows the synthetic data obtained from the forward model and the red line shows the adjusted data obtained by the 2D inversion model.

Figure 4 shows the semi-log plot of the convergence of the inverse model (F versus Generation), where F is the Goal Function, given by Equation 5.

$$F = \sqrt{(\rho_{ap_e} - \rho_{ap_o})^2 + (\phi_e - \phi_o)^2} \tag{5}$$

where ρ_{ap_e} is the estimated apparent resistivity, ρ_{ap_o} is the apparent resistivity observed (synthetic data), ϕ_e is the estimated phase and ϕ_o is the observed phase (synthetic data).

As we can see from Figure 4, the one hundred thousand generations used were sufficient for the convergence of the output parameters of the inverse model.

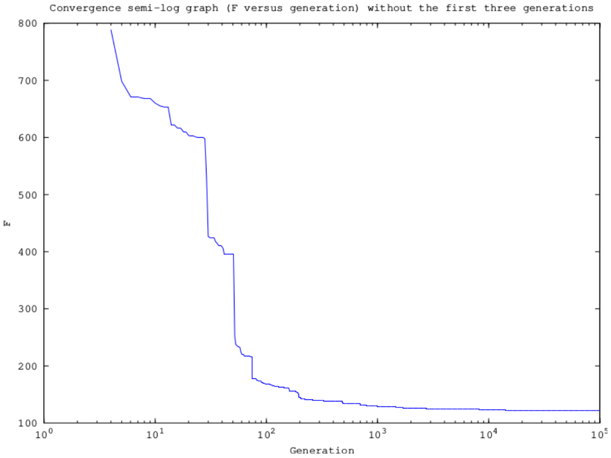

Figure 4: Convergence Graph

Table 2 shows the output parameters of the inverse model, containing the position of each of the 6 stations, the thicknesses of each of the layers and the values of their respective resistivities. With the data in Table 2, the profile of the inverse model used was made, as shown in Figure 5. The red filled circles located at the top of the profile correspond to the positions of the six stations. This profile was constructed in a manner analogous to that of the forward model profile, from left to right.

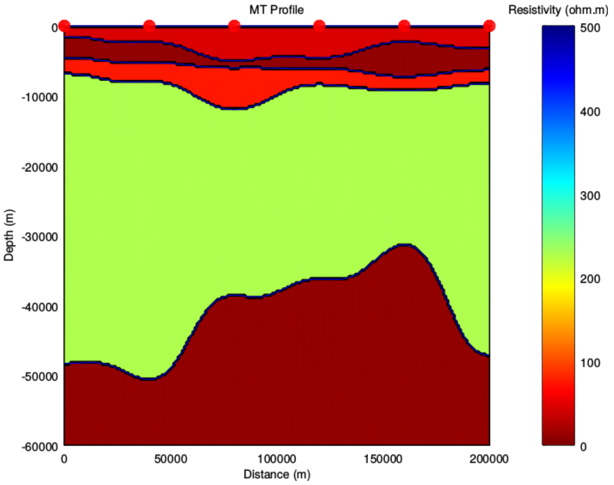

Figure 5: Profile of the inverse model

By comparing the profile of the forward model with that of the inverse model (see Figure 6), and by comparing the data from Table 1 with those from Table 2, we can observe that although layer 2 presents discrepancies regarding its shape after inversion, The other layers follow the thickness pattern presented in the forward model, especially layers 4 and 5. Regarding resistivities, layers 2 and 3 presented the highest discrepancy after inversion, however the other layers presented reasonable values, especially layers 1 and 5.

Table 2: Inverse model output.

		STATION 1	STATION 2	STATION 3	STATION 4	STATION 5	STATION 6
	HORIZONTAL COORDINATE (m)	0	40000	80000	120000	160000	200000
	RESISTIVITY $(\Omega.m)$	THICKNESS					
LAYER 1	47.26	1557.62	2303.96	4991.46	4563.52	2274.57	3250.19
LAYER 2	9.46	3017.84	2977.96	1011.12	1526.63	4981.72	3045.11
LAYER 3	77.01	2297.77	2704.40	5990.68	2302.90	2007.14	2000.65
LAYER 4	228.96	41435.71	42609.44	26567.56	27830.00	22063.36	38819.76
LAYER 5	9.74	∞	∞	∞	∞	∞	∞

Conclusions

The results obtained were satisfactory and indicate that the developed methodology has the potential to be applied in the study of sedimentary basins. One of the future prospects for this work is to perform the inversion with real data obtained by the Observatório Nacional in a NW-SE profile at the Parnaiba basin.

References

BERDICHEVSKY, M. N.; DMITRIEV, V. I. 2010. Models and Methods of Magnetotellurics. Springer Science & Business Media.

CHAVE, A. D.; JONES, A. G. 2012. The magnetotelluric method: Theory and practice. Cambridge University Press.

GOLDBERG, D. E. 1989. Genetic Algorithms in Search, Optimization and Machine Learning (1st ed.). Addison-Wesley Longman Publishing Co., Inc., Boston, MA, USA.

LINDEN, R. 2006. Algoritmos Genéticos. Rio de Janeiro: Brasport.

LUGÃO, P. P. 1993. Estudo Magnetotelúrico na Borda Leste da Bacia do Recôncavo; BA. Tese de Mestrado, Rio de Janeiro — RJ.

NUNES, H. O. 2007. Estudos Geofísicos e Tectonicos na Provincia Borborema. Relatório Final — INPE.

RIJO, L. 2004. Electrical Geophysics 1-D Earth Direct Modeling. [S.I.:s.n.].

SIMPSON, F.; BAHR, K. 2005. Practical magnetotellurics. Cambridge University Press.

Acknowledgments

Thanks to Prof. Dr. Emanuele Francesco La Terra for having made available the pre-processed data, information on the geology of the Parnaiba Basin and guidance for the use of WinGLink software that will be used in the future stages of this work. We also thank the Observatório Nacional for the structure made available to the work and the CNPq for the research funding.

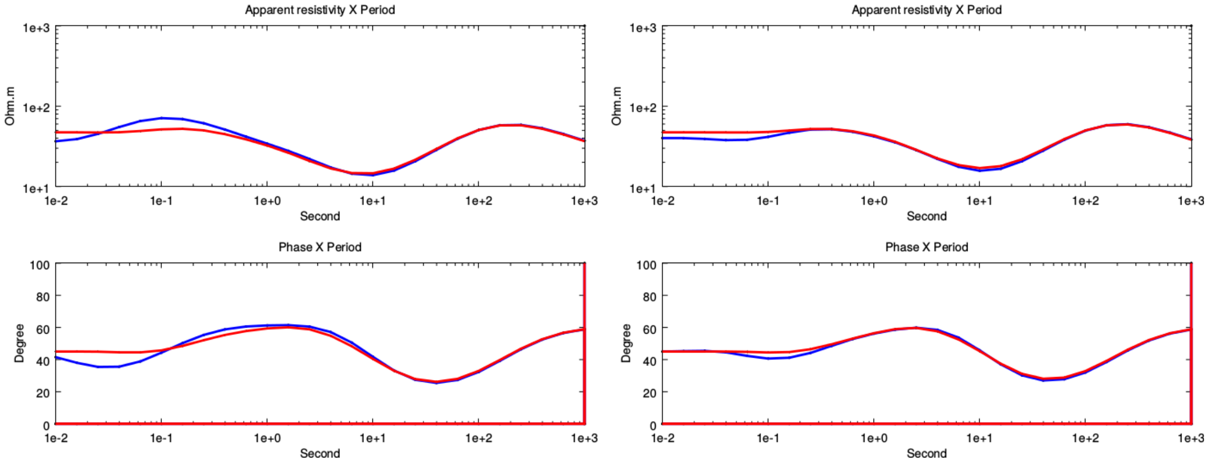

(a) Station 1 (b) Station 2

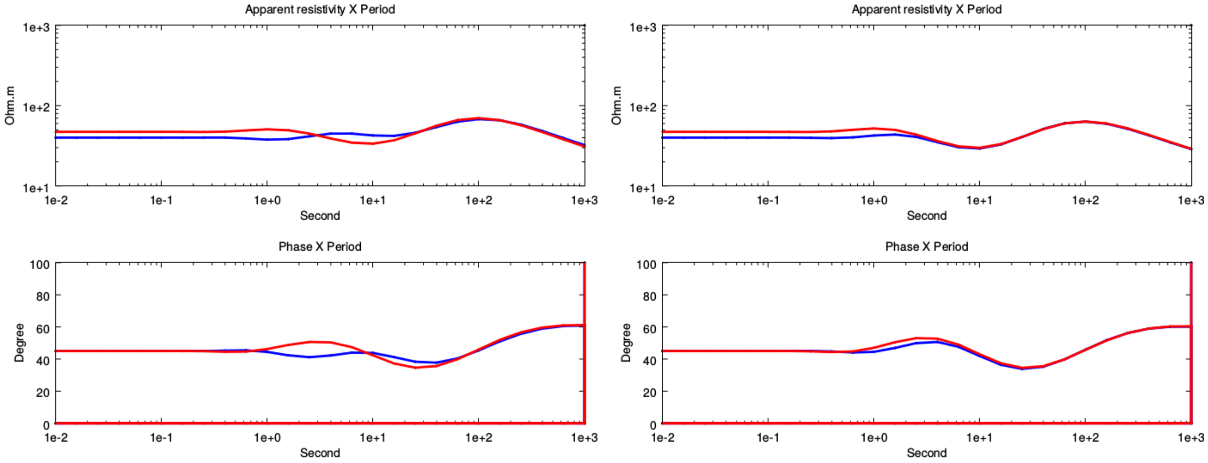

(c) Station 3 (d) Station 4

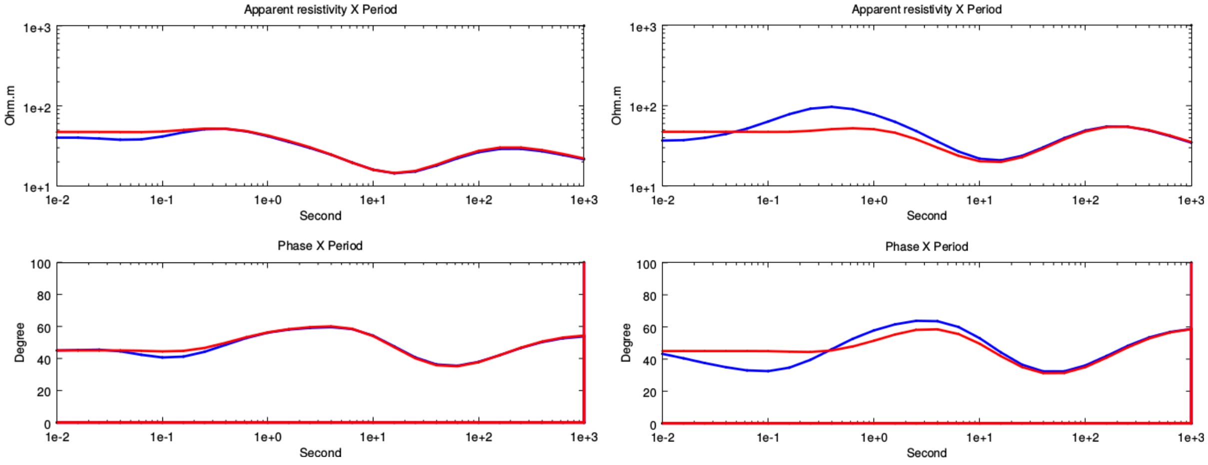

(e) Station 5 (f) Station 6

Figure 3: Fit graphs of all six stations.

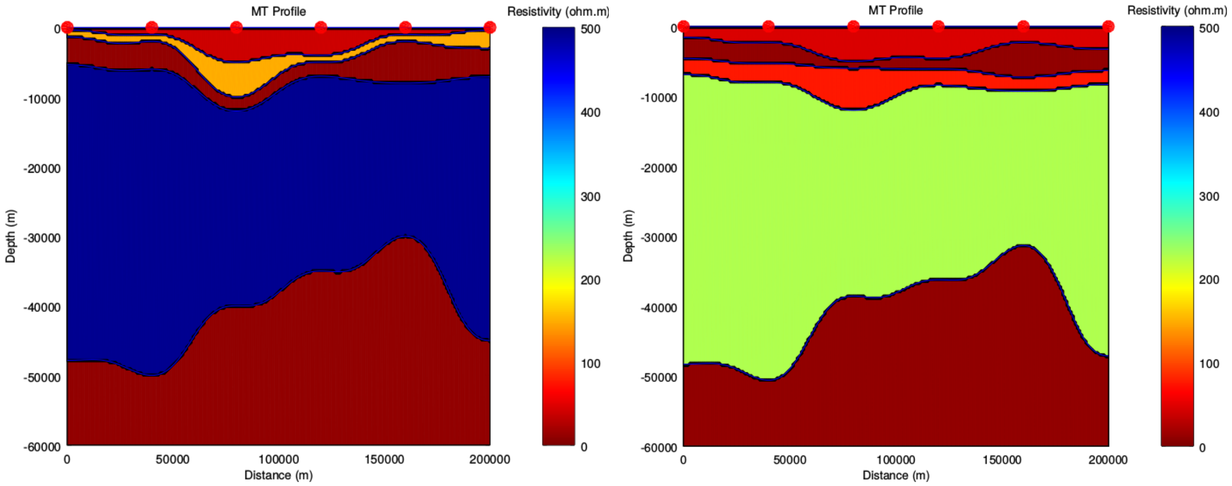

(a) Profile of the forward model

(b) Profile of the inverse model

Figure 6: Comparison of the profile of the forward model with the profile of the inverse model.